Volcanic hybrid earthquakes that are brittle-failure events

Rebecca M. Harrington[1] and Emily E. Brodsky[2]

Received 7 November 2006; revised 17 January 2007; accepted 5 February 2007; published 28 March 2007.

[1] Volcanoes generate a variety of pre-eruptive low-frequency seismic signals. Hybrid earthquakes comprise a class of these signals having high-frequency onsets followed by low-frequency ringing. They are used empirically to predict eruptions, but their ambiguous physical origin limits their diagnostic use. The short-duration, near-field hybrid seismograms associated with the 2004 Mount St. Helens eruption indicate that much of the prolonged signal is due to path rather than resonating fluids. We show using seismic source spectra that the hybrids have a corner frequency/seismic moment relationship that scales consistently with brittle-failure. The unusually low frequency of these earthquakes can result from low rupture velocities combined with strong path effects due to their shallow sources. This new application of near-field instrumentation provides the first seismological evidence for brittle-failure as a major process in dome building, and suggests that hybrids should not be used as direct indicators of fluids. **Citation:** Harrington, R. M., and E. E. Brodsky (2007), Volcanic hybrid earthquakes that are brittle-failure events, *Geophys. Res. Lett.*, *34*, L06308, doi:10.1029/2006GL028714.

1. Introduction

[2] Volcanic earthquakes are commonly categorized by frequency content to distinguish possible physical sources [*Lahr et al.*, 1994; *Chouet*, 1996; *Neuberg et al.*, 2000; *McNutt*, 2005]. Much work focuses on low-frequency earthquakes, as they are the most poorly understood and most distinctive of volcanic systems. Prolonged ringing of ground motions at frequencies $\sim$1 Hz distinguishes them from typical high-frequency volcano tectonic earthquakes, and is often thought to result from either moving fluids or a resonating, fluid-filled conduit [*Julian*, 1994; *Lahr et al.*, 1994; *Chouet*, 1996; *Neuberg et al.*, 2000]. Hybrids are a subset of low-frequency earthquakes characterized by high-frequency onsets, which may represent a separate trigger that initiates conduit resonance [*Neuberg et al.*, 2006]. At some sites, hybrids form a continuum with pure low-frequency events and therefore may be due to the same mechanism [*Neuberg et al.*, 2000].

[3] Either fluids or path effects account for the low-frequency portion of hybrid waveforms. Their protracted durations could result from trapped waves in the soft, loosely consolidated upper layers of the volcanic edifice rather than a resonating fluid source [*Kedar et al.*, 1996]. Our goal is to distinguish path from source, and by extension, the origin of the unusual seismograms. To do this, we first investigate the scaling of duration with distance in a velocity record section. This simple observation itself will favor a path origin for much of the signal. We then use the Empirical Green's Function approach to remove path effects from the source time function in the seismic records at Mount St. Helens [*Nakanishi*, 1991]. We will find that the source duration scales with moment in a way that is typical for brittle-failure events. Finally, we will discuss the physical mechanisms that account for the unusual seismograms.

2. Data and Methods

[4] The current eruption at Mount St. Helens commenced in late September 2004 with a series of steam and ash explosions, followed by extrusion of multiple brittle rock spines with visible gouge that now form a new dome inside the crater [*Pallister et al.*, 2006]. The seismicity associated with the spine extrusions is characterized by shallow, periodic earthquakes, commencing with high frequency onsets and transitioning to codas with spectral peaks at 1–2 Hz and durations longer than is typical for earthquakes of the same magnitude in a standard tectonic setting. With the exception of the first week of activity, there is a lack of purely high-frequency volcano tectonic events, and the hybrid codas do not show the monochromatic peaked spectra found for some occurrences of volcanic tremor. The high-frequency onsets, and long-period, long-duration codas are features shared by hybrid earthquakes seen at other volcanoes such as Montserrat, Redoubt, and Deception Island [*Lahr et al.*, 1994; *Miller et al.*, 1998; *Neuberg et al.*, 2000; *Ibanez et al.*, 2003] (Figure 1). The data for volcanoes other than Mount St. Helens is limited, but the waveform similarity indicates that hybrid events are similar.

[5] The coda duration of the Mount St. Helens hybrids decreases sharply with distance, suggesting that some, if not all of the protracted duration is due to path effects rather than an extended source. A mantle of abraded gouge surrounds the base of the spines and shows many features seen in shallow fault zones [*Pallister et al.*, 2006]. Although we cannot definitively co-locate the seismic sources with gouge formation, contemporaneous seismic and acoustic data suggest that most of the earthquakes occur at or very near the surface [*Moran et al.*, 2005]. The decreasing coda durations with distance from the source and the presence of gouge at the base of the spines suggest that the seismicity associated with the spine extrusions could result from brittle failure between the spine and the surrounding rock.

[6] The seismograms in Figure 1 depict hybrids recorded at distances $\geq$1 km from their hypocenters; however, increased instrumentation at Mount St. Helens in early 2005 provides records as close as $\sim$100 meters from the active spine. The particularly hindering path effects in a

[1]Department of Earth and Space Sciences, University of California, Los Angeles, California, USA.
[2]Department of Earth and Planetary Sciences, University of California, Santa Cruz, California, USA.

0094-8276/07/2006GL028714

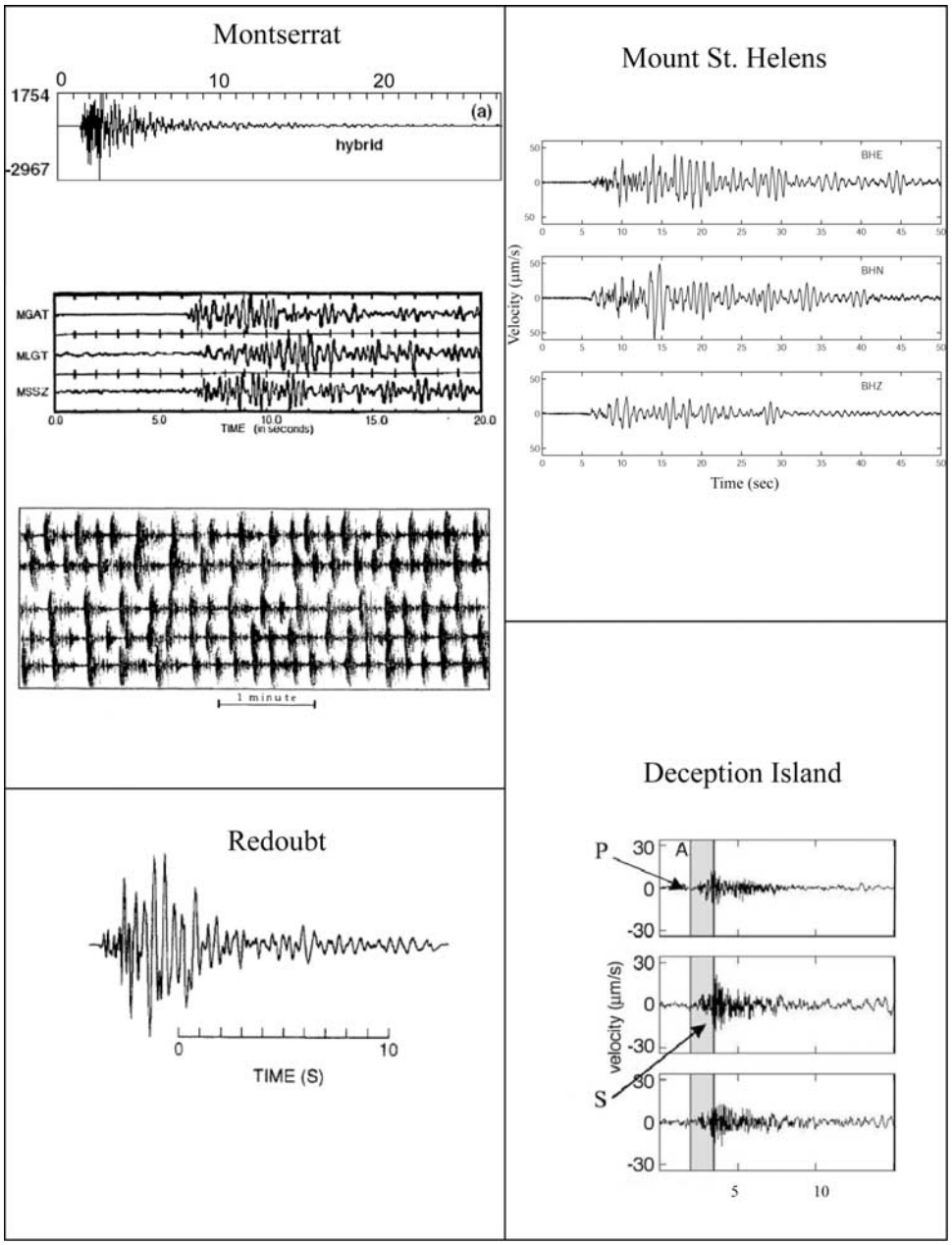

Figure 1. Seismograms for typical hybrid earthquakes at Mount St. Helens, Montserrat, Redoubt and Deception Island [*Chouet et al.*, 1994; *Ibanez et al.*, 2003; *Neuberg et al.*, 2000; *White et al.*, 1998]. No obvious differences are apparent between hybrid earthquakes at different volcanoes, suggesting that the physical processes causing these events are similar. (All stations recordings are $\geq$1 km from the earthquakes).

volcano make close stations crucial to analyzing earthquake source processes. For example, a record section of a M_L 1.1 event on February 26th, 2005 shows roughly an order of magnitude increase in recorded event duration with increasing station distance. Thus, the majority of the seismic signal at the $\sim$1–2 km distances typical of other deployments is generated along the path, probably through scattering (Figures 2 and S1[1]). The shaking duration of 3 seconds at the closest station, MIDE, provides an upper bound on source duration. Although substantially less than the 20-second duration seen at distant sites, it is still two orders of magnitude longer than typical source durations for ordinary earthquakes of this magnitude. The large scattering occurring farther out suggests that this prolonged source duration at MIDE is the result of attenuation, however, an extended source could also extend the signal. We evaluate this possibility using Figure 2.

[7] The increased duration of the waveform with increased distance implies the scattering attenuation is large. In fact, an amplitude decay by a factor $\sim 10^3$ between stations MIDE and JUN, at distances of 0.110, and 6.2 km from the crater, respectively, implies that scattering Q is approximately 10. As is common in scattering attenuation

[1]Auxiliary materials are available in the HTML. doi:10.1029/2006GL028714.

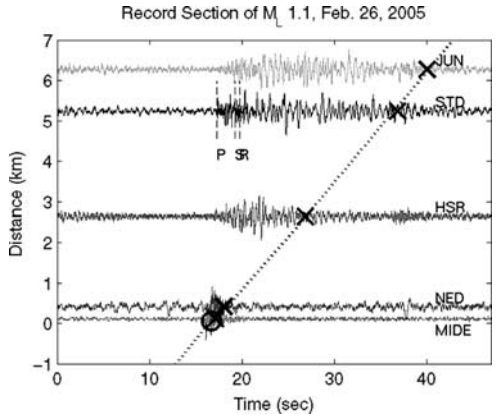

Figure 2. Seismic record section plot of a M_L 1.1 hybrid earthquake on February 26, 2005 in the crater at Mount St. Helens with instrument response removed. The velocity records are normalized by the peak of the trace. The plot shows duration lengthening with increasing distance from the crater. P-, S- and Rayleigh wave arrivals are annotated on the signal for STD (the only 3-component station shown), where Rayleigh waves were identified using particle motion plots with a band-pass filter of 0.5–2 Hz. The square at each station denotes the time duration required for the amplitude to decay to e^{-1} times the value of the peak amplitude (see text). The circle indicates the intersection of the trend with the source length as determined by the corner frequency.

studies, we assume that the duration of the coda increases linearly with distance, and extrapolate the trend to the source duration inferred from the moment estimation of the source-time function obtained from the Empirical Green's function deconvolution discussed below [*Aki and Richards*, 2002]. Using an e^{-1} decay time as a measurement of duration yields a duration of 0.9 s at a distance of 60 m. While this procedure does not determine the source duration directly, it is a tool to evaluate the extent to which path attenuation outside the conduit makes the source appear extended at the closest stations. Since a resonating conduit should extend the duration of the waveform as recorded near the source, the resonating waves can only account for at most an extension of 0.8 s in the signal. A resonating pipe is not producing the key features of this signal as observed at more typical stations distances of a few kilometers and therefore the extended durations in Figure 2 cannot be taken as evidence of a fluid-filled conduit. If all of the extended duration is a result of path, this would suggest that hybrids sources are no different than tectonic earthquake sources. To determine if hybrid sources scale like tectonic earthquakes, we isolate source spectra using an Empirical Green's Function approach.

[8] Because the Mount St. Helens hybrids have extremely similar waveforms and are likely located in nearly the same place along the extruding spine, they are well suited for using an Empirical Green's Function analysis. We deconvolve the smallest observable event with spectral amplitude visible above noise on station MIDE from the larger events on that station to obtain the source time functions of the larger events (example in Figure S2). Because we use events from the same station, we leave in the instrument response to avoid introducing noise through an extra, unnecessary deconvolution. We use the entire length of the larger event for the deconvolution in order to ascertain that the source-time function has effectively zero amplitude in the coda. Stations MIDE and NED in the Cascades Chain network are closest to the extruding spine, and therefore record the widest dynamic range of events. Using both high- and low-gain channels also increases the dynamic range of events used. We use the source-time functions obtained by the Empirical Green's Function deconvolution to fit the seismic moment and corner frequency of the source-time spectra using a least-squares curve fit to a f^2 spectrum [*Boatwright*, 1978; *Abercrombie*, 1995; *Ide et al.*, 2003],

$$\Omega(f) = \frac{\Omega_0}{\left[1 + (f/f_c)^4\right]^{1/2}} \quad (1)$$

where f_c is corner frequency, and Ω_0 is long period amplitude (Figure 3). We omitted the attenuation coefficient commonly seen in equation (1) because the Empirical Green's Function deconvolution removes these effects [*Nakanishi*, 1991].

[9] Another approach to constraining the source of these events would be moment tensor inversion. Previous research on low-frequency earthquakes suggested a source model involving fluid motion and therefore including some volumetric component [*Julian*, 1994; *Chouet*, 1996; *Neuberg et al.*, 2000]. A non-double couple source could in principle be identified through a full waveform inversion [*Chouet et al.*, 2003]. However, the site's limited near-field station coverage, unconstrained velocity structure, and significant scattering (Figure 2) would make obtaining stable focal mechanism solutions difficult [*Hardebeck and Shearer*, 2002]. An Empirical Green's function analysis, which can be performed with one station, and requires no assumption

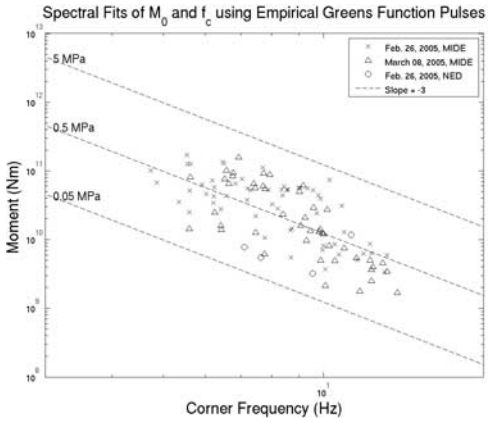

Figure 3. Logarithmic plot of M_0 vs. corner frequency, f_c, modeled from the source-time functions of the Mount St. Helens hybrids in 2005. Both high- and low-gain channels for stations MIDE and NED of the Cascades chain are used in the Empirical Green's Function deconvolution. A least-squares fit gives a slope of 3.3 ± 0.3, which is consistent with the standard model of a 2-D fault. Most of the earthquakes have stress drops of about 0.5 MPa, falling well within the typical range of values for earthquakes (0.1 to 100 MPa) [*Abercrombie*, 1995]. There are 108 events on this plot.

of velocity structure, is a more viable approach even though it does not recover the moment tensor.

[10] Earthquakes generated by a shear dislocation on a 2-D surface are mathematically equivalent to a distribution of double-couples with total moment proportional to the average slip multiplied by the fault area [*Burridge and Knopoff*, 1964]. The seismic moment for a planar fault is proportional to the product of the stress drop and the rupture length cubed. For a circular fault

$$M_0 = \frac{16}{7} a^3 \Delta\sigma \tag{2}$$

where a is the radius of the rupture. The source radius can be measured from seismograms using the corner frequency f_c and the relationship

$$a = 0.315\beta / f_c \tag{3}$$

which relates corner frequency to fault geometry, where β is the shear velocity [*Madariaga*, 1976]. Combining equations (2) and (3), implies that

$$M_0 \propto f_c^{-3} \tag{4}$$

if stress drop is size-independent. Although the constants in equations (2) and (3) are fault-geometry dependent, equation (4) is a robust relationship for double-couple events and is commonly observed for tectonic earthquakes [*Kanamori and Anderson*, 1975; *Abercrombie*, 1995]. Some of the hybrids, though not all (Figure S3) show the same polarity at all stations, which could suggest failure on a ring-shaped fault. However, because fault-geometry affects only the constants, stick-slip failure on this type of fault should still be governed by equation (4).

[11] Figure 3 shows that the correlation between the M_0 and f_c of the Mount St. Helens hybrids is consistent with the model of a standard 2-D fault. The corner frequency, f_c, is proportional to M_0 on a logarithmic plot with a slope of $-3.3 + -0.3$ (errors are 1 standard deviation of 10,000 bootstrap trials). Examples of the spectra on which the M_0, and f_c, values of Figure 3 are based are shown in Figure 4. Therefore, a source model of shear failure on a crack with constant stress drop is consistent with the data.

[12] Many models for hybrids focus on a resonating fluid-filled conduit as the source of the prolonged low-frequency waves. In the simplest model of a linear organ pipe, the frequency content of the signal is determined entirely by geometry and there is no reason that the amplitude (or moment) should scale with frequency in any particular relationship. *Julian* [1994] proposes a more complex model where the frequency of oscillation is dependent on the strength of the resonating wave due to a coupling between the fluid and elastic systems. However, even in this nonlinear oscillator, there is no reason that the amplitude (and moment) should scale according to the relationship in equation (4).

[13] Although the M_0/f_c relationship of the Mount St. Helens hybrids scales in the same way as typical earthquakes, the corner frequencies are lower than expected for a given moment. For example, the local moment magnitudes of the earthquakes in Figure 4 range from 0.2 to 1.5 and

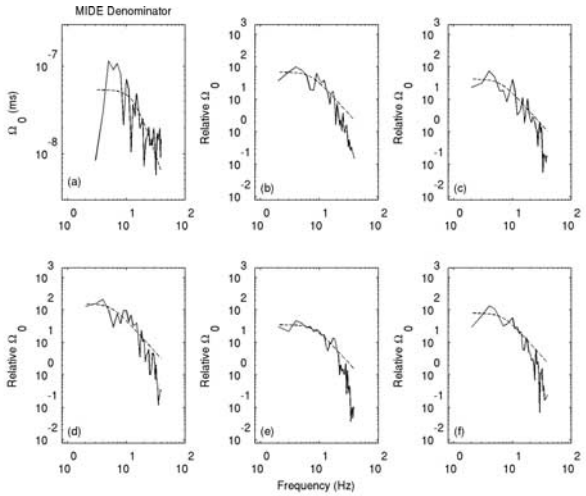

Event	M_w	M_0 (Nm)	Relative Ω_0	f_c (Hz)
(a)	0.07	1.5 X 10^9	--	13
(b)	1.1	5.5 X 10^{10}	69	7
(c)	1.0	3.4 X 10^{10}	42	6
(d)	1.3	1.3 X 10^{11}	156	6
(e)	0.9	2.8 X 10^{10}	35	8
(f)	1.1	6.5 X 10^{10}	81	7

Figure 4. (a) Example of a small event used as the denominator in spectral division (Empirical Green's function analysis) for the February 2005 events at station MIDE. The absolute moment of this event gives the moment of each event using the relative value of Ω_0. (b–f) Examples of source time function spectra; solid lines are data, and dashed lines are the fit of equation (1). Figure 4b is the event shown in Figure 2. The table indicates the values obtained from the fit of equation (1).

corner frequencies range from 5 to 14 Hz, whereas corner frequencies for tectonic earthquakes in this magnitude range are more on the order of tens of Hz [*Abercrombie*, 1995; *Ide et al.*, 2003]. These low corner frequencies can be explained by low rupture velocities.

[14] Earthquake locations and time-lapse photographs of concurrent motion suggest that the earthquakes occur on the rock spine in the crater [*Moran et al.*, 2005]. This unusual situation constrains the absolute hypocenter of the earthquakes and therefore provides a method to measure the seismic wave velocities. Using S-P arrival time and the relation between P and S velocity in a Poisson solid, we calculate the P- and S-velocity in the path to that station. Repeating this for all of the stations within 5 km produces an average value of 700 m/s for the S-velocity, β. Rayleigh wave velocity, which has a half-space value of 0.9β, generally limits rupture velocity. This calculation implies a rupture velocity of 650 m/s or less, much lower than typical values of 2–3 km/s at ordinary tectonic sites. The low rupture velocity is the origin of the apparently low corner-frequency of the hybrids, and this combines with strong scattering in the heterogeneous volcanic crust to yield the unusual hybrid seismograms.

[15] Our analysis clearly indicates a source with a spectral scaling consistent with brittle failure. However, if some part of the waveform for each event results from a simple, entirely repeatable resonating cavity, it would be removed as part of the Green's function. Thus, it is possible that the

source spectra of Figure 4 are only part of the source. However, we already showed that the prolonged seismogram results primarily from scattering consistent with Q $\approx$ 10. Thus any contribution of a resonating cavity must be $\leq$0.8 seconds, rather than the 25 seconds seen at 6 km.

[16] Figure 3 implies the self-similarity of earthquakes down to M_w 0.2 (the smallest magnitude shown). By combining equations (2) and (3), we see that fitting a straight line to the data in Figure 3 requires that the quantity $\delta\sigma\beta^3$ must be constant. There is no compelling reason to assume that either β or rupture velocity varies dramatically with size, and hence no reason to assume that stress drop does either. This self-similarity for small earthquakes is consistent with results shown by *Abercrombie* [1995], however we are able to extend these results down to a smaller magnitude.

3. Conclusions

[17] In summary, the Mount St. Helens earthquakes produce unusual seismograms typical of volcanic hybrids, yet our analysis shows that their M_0/f_c relationship is consistent with standard tectonic earthquakes and might be explained simply by brittle- failure in combination with a very complicated path and low rupture velocities. This seismic evidence for the prevalence of brittle failure events favors new eruptive models that use stick-slip failure as the primary mechanism of dome growth [*Iverson et al.*, 2006]. Furthermore, the data imply that earthquakes are scale invariant down to M_w 0.2 with typical stress drops of $\sim$0.5 MPa. We note that extending this result to deeper hybrid events would require the analysis of a different data set, as all of the hybrid earthquakes at Mount St. Helens occurred at or near the surface.

[18] Hybrid earthquakes occur at many volcanoes, and are often precursors to explosive eruption. The continuum of frequency spectra between hybrids and other low-frequency events implies that all of these types of earthquakes may share the same type of mechanism [*Neuberg et al.*, 2000]. Our study shows that in some cases hybrids are consistent with brittle failure, suggesting that fluids are no more necessary to explain the generation of these seismic waves than to explain ordinary earthquakes. Therefore, hybrid earthquakes on volcanoes do not directly and definitively indicate the movement of a free fluid. In some cases hybrids reflect fault failure in the volcanic edifice resulting from magma movement and/or pressurization and thus are indirect indicators of magma, and hence impending eruptions. However, other stresses, such as gravity, could potentially cause shallow earthquakes with protracted waveforms, so the mere presence of hybrids unfortunately does not mean that magma is on the move.

[19] **Acknowledgments.** The seismic data used here was collected by the Cascades Volcano Observatory (CVO) and the Pacific Northwest Seismograph Network (PNSN), and distributed by the Incorporated Research Institutions for Seismology (IRIS) Consortium. This work was funded in part by the National Science Foundation. We thank Thorne Lay for the use of his empirical Green's function code and several helpful discussions. We thank Seth Moran and the staff at CVO for their extensive support during the ongoing eruption, and many valuable insights.

References

Abercrombie, R. E. (1995), Earthquake source scaling relationships from −1 to 5 ML using seismograms recorded at 2.5-km depth, *J. Geophys. Res.*, *100*(B12), 24,015–24,036.

Aki, K., and P. G. Richards (2002), *Quantitative Seismology*, 2nd ed., 700 pp., Univ. Sci., Sausalito, Calif.

Boatwright, J. (1978), Detailed spectral analysis of 2 small New-York-state earthquakes, *Bull. Seismol. Soc. Am.*, *68*, 1117–1131.

Burridge, R., and L. Knopoff (1964), Body force equivalents for seismic dislocations, *Bull. Seismol. Soc. Am.*, *54*, 1875–1888.

Chouet, B. A. (1996), Long-period volcano seismicity: Its source and use in eruption forecasting, *Nature*, *380*, 309–316.

Chouet, B. A., R. A. Page, C. D. Stephens, J. C. Lahr, and J. A. Power (1994), Precursory swarms of long-period events at Redoubt volcano (1989–1990), Alaska—Their origin and use as a forecasting tool, *J. Volcanol. Geotherm. Res.*, *62*, 95–135.

Chouet, B., P. Dawson, T. Ohminato, M. Martini, G. Saccorotti, F. Giudicepietro, G. De Luca, G. Milana, and R. Scarpa (2003), Source mechanisms of explosions at Stromboli Volcano, Italy, determined from moment-tensor inversions of very-long-period data, *J. Geophys. Res.*, *108*(B1), 2019, doi:10.1029/2002JB001919.

Hardebeck, J. L., and P. M. Shearer (2002), A new method for determining first-motion focal mechanisms, *Bull. Seismol. Soc. Am.*, *92*, 2264–2276.

Ibanez, J. M., E. Carmona, J. Almendros, G. Saccorotti, E. Del Pezzo, M. Abril, and R. Ortiz (2003), The 1998–1999 seismic series at Deception Island volcano, Antarctica, *J. Volcanol. Geotherm. Res.*, *128*, 65–88.

Ide, S., G. C. Beroza, S. G. Prejean, and W. L. Ellsworth (2003), Apparent break in earthquake scaling due to path and site effects on deep borehole recordings, *J. Geophys. Res.*, *108*(B5), 2271, doi:10.1029/2001JB001617.

Iverson, R. M., et al. (2006), Dynamics of seismogenic volcanic extrusion at Mount St. Helens in 2004–05, *Nature*, *444*, 439–443.

Julian, B. R. (1994), Volcanic tremor: Nonlinear excitation by fluid flow, *J. Geophys. Res.*, *99*(B6), 11,859–11,878.

Kanamori, H., and D. L. Anderson (1975), Theoretical basis of some empirical relations in seismology, *Bull. Seismol. Soc. Am.*, *65*, 1073–1095.

Kedar, S., B. Sturtevant, and H. Kanamori (1996), The origin of harmonic tremor at Old Faithful Geyser, *Nature*, *379*, 708–711.

Lahr, J. C., B. A. Chouet, C. D. Stephens, J. D. Power, and R. A. Page (1994), Earthquake classification, location, and error analysis in a volcanic environment—Implications for the magmatic system of the 1989–1990 eruptions at redoubt volcano, Alaska, *J. Volcanol. Geotherm. Res.*, *62*, 137–151.

Madariaga, R. (1976), Dynamics of an expanding circular fault, *Bull. Seismol. Soc. Am.*, *66*, 639–666.

McNutt, S. R. (2005), Volcano seismology, *Annu. Rev. Earth Planet. Sci.*, *33*, 461–491.

Miller, A. D., R. C. Stewart, R. A. White, R. Luckett, B. J. Baptie, W. P. Aspinall, J. L. Latchman, L. L. Lynch, and B. Voight (1998), Seismicity associated with dome growth and collapse at the Soufriere Hills Volcano, Montserrat, *Geophys. Res. Lett.*, *25*(18), 3401–3404.

Moran, S. C., A. I. Qamar, and H. M. Buurman (2005), Automated earthquake detection during the 2004–2005 eruption of Mount St. Helens, *Eos Trans. AGU*, *86*(52), Fall Meet. Suppl., Abstract V53D-1600.

Nakanishi, I. (1991), Source process of the 1989 Sanriku-Oki earthquake, Japan—Source function determined using empirical Green-function, *J. Phys. Earth*, *39*(6), 661–667.

Neuberg, J., R. Luckett, B. Baptie, and K. Olsen (2000), Models of tremor and low-frequency earthquake swarms on Montserrat, *J. Volcanol. Geotherm. Res.*, *101*, 83–104.

Neuberg, J. W., et al. (2006), The trigger mechanism of low-frequency earthquakes on Montserrat, *J. Volcanol. Geotherm. Res.*, *153*, 37–50.

Pallister, J. S., R. Hoblitt, R. Denlinger, D. Sherrod, K. Cashman, C. Thornber, and S. Moran (2006), Structural geology of the Mount St. Helens fault-gouge zone—Field relations along the volcanic conduit wallrock interface, *Eos Trans. AGU*, *87*(52), Fall Meet. Suppl., Abstract V41A-1703.

White, R. A., A. D. Miller, L. Lynch, and J. Power (1998), Observations of hybrid seismic events at Soufriere Hills Volcano, Montserrat: July 1995 to September 1996, *Geophys. Res. Lett.*, *25*(19), 3657–3660.

E. E. Brodsky, Department of Earth and Planetary Sciences, University of California, 1156 High St., Santa Cruz, CA 95060, USA.

R. M. Harrington, Department of Earth and Space Sciences, University of California, 595 Charles Young Drive East, 3806 Geology Building, Los Angeles, CA 90095-1567, USA. (rebecca@moho.ess.ucla.edu)